Sequence-dependent force response during peeling of single-stranded DNA from graphite

Suresh Manohar[1] and Anand Jagota[1,2,*]
[1]*Department of Chemical Engineering, Lehigh University, Bethlehem, Pennsylvania 18015, USA*
[2]*Bioengineering Program, Lehigh University, Bethlehem, Pennsylvania 18015, USA*
(Received 27 March 2009; revised manuscript received 26 November 2009; published 23 February 2010)

We have analyzed the statistical thermodynamics of peeling single-stranded DNA (ssDNA) from the surface of graphite. Using recently measured parameters, we represent ssDNA as a polymer chain strongly adsorbed to a frictionless substrate using the freely jointed chain, wormlike chain, and rotational isomeric state models. All three models predict steady peeling force under force control, in agreement with single-molecule experiments. We predict that, for finite-length chains, the force response has measurable spikes under displacement control. These force spikes carry information about the underlying sequence of ssDNA, which might thus be measurable with a sufficiently stiff loading system. For the freely jointed chain model, under force control, we have obtained several exact closed-form results and provide relations between the measured peel force and the underlying adhesion free energy.

DOI: 10.1103/PhysRevE.81.021805 PACS number(s): 36.20.−r, 82.37.Rs

I. INRODUCTION

In recent years, single-molecule force spectroscopy, for example, using optical tweezers [1,2] and atomic force microscopy [3–5], has added greatly to our understanding of the mechanical behavior of polymer chains and has provided some of the best validation for idealized models such as the freely jointed chain (FJC) and the wormlike chain (WLC) [1,3,6,7]. Several experiments in which (usually) long molecules are adsorbed onto and then peeled off a substrate show that often peeling of a single polymer chain occurs at a steady force prior to its complete detachment [3–5,8–12]. This is analogous to the conventional peeling of thin films from a rigid substrate [13]. This technique has recently been used to measure forces required to peel short strands (50 bases) of single-stranded DNA (ssDNA) adsorbed onto graphite [14]. Consistent with previous adsorption measurements [15,16], it was found that the adsorption is strong (8–12 k_BT/base at $T=300$ K) and that there are significant base-to-base differences in adhesion free energy (e.g., T-11.5 k_BT; C-8.3 k_BT at $T=300$ K).

Simple energy balance models [5,9,10] have been developed to relate the force required to peel the polymer from the substrate and the adhesion free energy between the two. Several existing models treat the desorbed polymer as an approximate Gaussian chain [5,10,17] which is valid only for small chain extensions, whereas, in most cases, the desorbed polymer is stretched a significant fraction of its contour length. Previous models have not studied the statistics of the peeling process in significant detail, nor considered whether peeling of finite-length chains differs depending on whether it is done under force control (FC) or displacement control (DC).

Single molecule *stretching* experiments have provided an unprecedented view on the mechanics of single molecules, for example, how secondary or tertiary structure in a biological molecule evolves under increasing stretch [1,2,18,19]. An intriguing open question remains: potentially what level of detail could a single-molecule *peeling* experiment provide about the interaction between individual groups and a surface?

In this paper, we consider the specific example of ssDNA peeled from graphite, which we analyze as the peeling of a strongly adsorbed polymer chain from a frictionless substrate. (This corresponds well to the character of ssDNA adsorption on graphite [14]; it also applies in several other instances [5,10–12].) The behavior of the ssDNA chain is described by three polymer models, namely, FJC, WLC, and rotational isomeric state (RIS) models. All three predict that, for short strands, the force-displacement relation depends on the ensemble (FC vs DC). The FC ensemble model predicts peeling to occur at a steady force [3–5,8–12,14], and provides the *relation* between the *adhesion free energy of a monomer* and the *peeling force*. Under DC, we predict *base-by-base* peeling with spikes in force characteristic of the adsorbing base, suggesting that the ssDNA *sequence* could be read thus with a sufficiently stiff loading system. The simple FJC model has been analyzed in greater detail, yielding several exact closed-form solutions.

The remainder of the paper is organized as follows. We present the model and its assumptions in Sec. II, and provide the reference result that relates steady peel force of a homopolymer under FC to the adhesion free energy. In Sec. III, we formulate the statistical thermodynamics of peeling under FC and DC; its results are presented in Sec. IV. We close with a summary and conclusions in Sec. V.

II. STATISTICAL THERMODYNAMICS OF PEELING

A. Schematic representation of peeling of ssDNA

Figure 1(a) depicts the peeling of an ssDNA molecule from a frictionless substrate by the application of a force, f, or a displacement, R_z. The ssDNA molecule has N mers [Fig. 1(b)], and each mer of contour length l_m has a backbone with six bonds and a base (adenine, guanine, cytosine, or thymine). The numbers of desorbed and adsorbed mers (or bases)

*Corresponding author; anj6@lehigh.edu

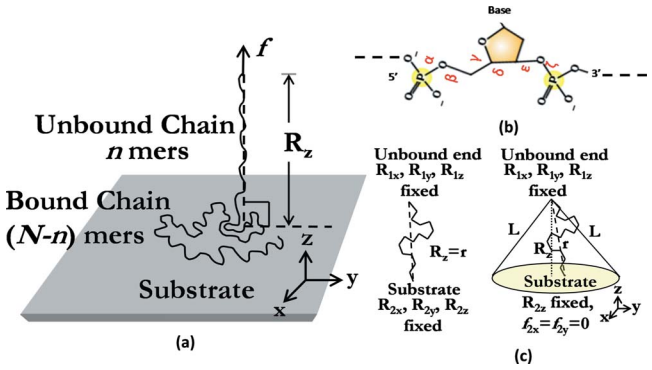

FIG. 1. (Color online) (a) Schematic representation of peeling an ssDNA molecule off graphite. (b) One mer of ssDNA with six backbone torsion angles. (c) In strict-displacement control (left), both ends of ssDNA are fixed. In semidisplacement control (right), the end away from the substrate is fixed while the adsorbed end maintains a fixed distance along the z direction (R_z) and remains free to move in the x-y plane since the substrate is frictionless.

are n and $(N\text{-}n)$, respectively, and γ is the adhesion free energy per unit contour length of the backbone chain. Each adsorbed mer decreases the free energy by γl_m. We represent the stretching behavior by three idealized polymer chain models: (i) FJC, (ii) WLC, and (iii) rotational isomeric state (RIS). Based on these models, we formulate the statistical thermodynamics for peeling of ssDNA from graphite with the following assumptions.

(a) Peeling occurs in equilibrium, i.e., over the time scale of the experiment the chain samples all conformations, and links go freely in and out of adhesive contact [9,10,12,14].

(b) The adsorption is strong—all $(N\text{-}n)$ links are adsorbed. The very end of the chain is constrained to remain on the substrate. This artifact is introduced to remove the nonequilibrium event of complete chain detachment.

(c) The substrate is frictionless; it cannot transmit any in-plane forces.

Assumption (a) is justified by the rate-independence of peel force; (b) is justified *a posteriori* by the measured adsorption free energy, which is found to be large compared to k_BT per Kuhn length; and (c) is based on observations that the force resisting sliding is immeasurably small, and simulations that show that the barrier for diffusion of surface bound nucleotides is on the order of k_BT [9,10,12,14].

B. Freely jointed chain model

In the FJC model, ssDNA is represented by N Kuhn links where each link has length b and adsorbed adhesion free energy γb. From our previous stretching experiments on short strands of ssDNA [14], we obtained Kuhn length in the range 0.51–1.0 nm, significantly smaller than the ~1.6 nm value reported for long strands [1,2]. For the results reported in this paper, we have used $b=l_m=0.69$ nm (where l_m is the contour length of one mer, see details in RIS model). With this, one base is assigned to one Kuhn link in the FJC, i.e., γb=single base adhesion energy. This allows us to compare the three models conveniently; our conclusions are not altered for different choices of b within the experimentally determined range.

A simple argument that balances work and desorbed chain free energy with the adhesion free energy of the adsorbed chain produces the result that under FC peeling occurs under constant force [3–5,8–12,14]. For an FJC, the measured constant force f^* is related to the adhesion γ [14] by

$$\gamma = \left(\frac{k_BT}{b}\right)\ln\left[\frac{4\pi\sinh(f^*b/k_BT)}{(f^*b/k_BT)}\right];$$

$$\Gamma = X^* \tag{1}$$

where the second form is in terms of dimensionless adhesion free energy Γ and dimensionless force F^*,

$$\Gamma = \frac{\gamma b}{k_BT}, \quad X^* = \ln\left[\frac{4\pi\sinh F^*}{F^*}\right] \text{ and } F^* = f^*b/k_BT. \tag{2}$$

Equation (1) is the limiting behavior for large N and n of more complete statistical models under FC ($T\gamma f$ ensemble) and DC ($T\gamma R_z$ ensemble), which we develop below.

1. Force control ($T\Gamma F$ ensemble)

Consider that the FJC is subjected to a given force f [Fig. 1(a)]. The chain responds by desorbtion of n links, where n can vary from 0 to N. The conformational partition function of an FJC with n desorbed links is the product of the well-known partition function for an FJC [6,7,20–22], $Z_F^{FJC}(n,F)$, and that of the adsorbed part of the chain, $Z_{ads}(n)$. The total partition function, $Z_{FC}^{FJC}(F)$, is the summation of this product over all allowed values of n (see also SI Sec. I [23]):

$$Z_{FC}^{FJC}(F) = \sum_{n=0}^{N} Z_{ads}(n) Z_F^{FJC}(n,F),$$

$$Z_{ads}(n) = \prod_{i=n}^{N} \exp(\Gamma_{i+1}),$$

$$Z_F^{FJC}(n,F) = \left(\frac{4\pi\sinh(F)}{F}\right)^n = \exp(nX),$$

$$P(n) = Z_{ads}(n) Z_F^{FJC}(n,F)/Z_{FC}^{FJC}, \tag{3}$$

where Γ_i is the dimensionless adhesion free energy of the i_{th} link, $\Gamma_{N+1}=0$, representing the case when all links are desorbed, and $P(n)$ is the probability of desorption of n links. Equation (3) admits conformations of the chain that penetrate the substrate, which allows us to obtain closed-form analytical results in some cases. By numerical calculations (SI Sec. II [23]) we have shown that for strongly adsorbing chains this approximation causes negligible error.

2. Displacement control ($T\Gamma R_z$ ensemble)

Under DC, the locations of the ends of the desorbed chain are held fixed. We consider two versions of DC [Fig. 1(c)]: (1) strict-DC, where both the ends of desorbed chain are fixed at a distance R_Z and (2) semi-DC, where the end away

from the substrate is fixed at a distance R_Z from it, whereas the adsorbed end is free to move in the x-y plane since its interaction with the substrate is frictionless.

The total partition function under DC is constructed in terms of the well-known probability distribution function (per unit volume) for an FJC with fixed number of links n to have two given end points separated by a distance r — $W(n,r)$ [6,7,21,22].

$$W(n,r) = (8\pi r b^2)^{-1} n(n-1) \sum_{t=0}^{\tau} \frac{(-1)^t}{t!\,(n-t)!} \left[\frac{n-(r/b)-2t}{2} \right]^{n-2}, \tag{4}$$

where τ is specified by $[(n\text{-}r/b)/2]\text{-}1 \le \tau < (n\text{-}r/b)/2$. In strict-DC, the partition function for fixed n and given R_z is $Z_F^{FJC}(n,0)W(n,R_z) = (4\pi)^n W(n,R_z)$ [7]. Semi-DC, on the other hand, requires one to integrate all the states in the x-y plane on the substrate, shown in the shaded region of Fig. 1(c). The total partition function in DC is therefore obtained as

$$Z_{DC}^{FJC}(R_Z) = \sum_{n=0}^{N} Z_{ads}(n) Z_R^{FJC}(n,R_Z),$$

$$Z_R^{FJC}(n,R_Z) = \begin{cases} (4\pi)^n W(n,R_z) & strict-DC \\ (4\pi)^n \displaystyle\int_{R_Z}^{L} W(n,r) 2\pi r dr & semi-DC \end{cases}. \tag{5}$$

Note that the apparent inconsistency in dimensions between strict-DC and semi-DC is of no consequence as far as calculation of force is concerned. A small constant area is implied in the former case that vanishes when one takes the derivative of the logarithm of partition function.

Our principal focus in this paper is on the use of the FJC model to study peeling under FC and DC. However, to establish the robustness of our main conclusions, we have also analyzed some cases of peeling using an approximate WLC and an RIS model to represent the desorbed part of the ssDNA.

C. Wormlike chain model

An ssDNA backbone with N mers is modeled as a WLC with persistence length l_p and contour length $l_c = N n_{pp} l_p$, where $n_{pp} = l_m / l_p$ is the number of persistence lengths per contour length of one mer. The partition function of a WLC is not known exactly but a good approximate relation that describes the force-extension behavior under DC is known, which we use to derive an approximate expression for free energy.

1. Displacement control

The approximate force-extension relation for a WLC is given by [24,25]

$$f(R_Z, l_c) = \frac{k_B T}{l_p} \left[\frac{1}{4} \left(1 - \frac{R_Z}{l_c} \right)^{-2} - \frac{1}{4} + \frac{R_Z}{l_c} \right], \tag{6}$$

where f is the average force on the chain with end-to-end distance R_z and contour length $l_c = n n_{pp} l_p$. Rewriting Eq. (6) in terms of dimensionless force F and dimensionless end-to-end distance $\overline{R_Z}$, we have

$$F(\overline{R_Z}, n) = n_{pp} \left[\frac{1}{4} \left(1 - \frac{\overline{R_Z}}{n} \right)^{-2} - \frac{1}{4} + \frac{\overline{R_Z}}{n} \right], \tag{7}$$

where $F = \frac{f n_{pp} l_p}{k_B T} = \frac{f b}{k_B T}$ and $\overline{R_Z} = \frac{R_Z}{n_{pp} l_p} = \frac{R_Z}{b}$. The area under the force-extension curve gives the free energy G of the chain, which in turn is equal to negative $k_B T$ times the natural logarithm of the partition function under DC. Therefore, the partition function at a given end-to-end distance R_z is given as

$$\begin{aligned} Z^{WLC}(n,\overline{R_Z}) &= (4\pi)^n \exp\left(-\frac{G}{kT} \right) \\ &= (4\pi)^n \exp\left\{ -n_{pp} \left[\frac{n}{4} \left(1 - \frac{\overline{R_Z}}{n} \right)^{-1} \right.\right. \\ &\quad \left.\left. - \frac{\overline{R_Z}}{4} + \frac{\overline{R_Z}^2}{2n} - \frac{n}{4} \right] \right\}. \end{aligned} \tag{8}$$

The constant factor, $(4\pi)^n$, ensures that the partition function matches that of an FJC at zero end-to-end distance. Similar to Eq. (5) for an FJC, the total partition function under DC is

$$Z_{DC}^{WLC}(\overline{R_Z}) = \sum_{n=0}^{N} Z_{ads}(n) Z^{WLC}(n,\overline{R_Z}). \tag{9}$$

2. Force control

The partition function under force control can be determined from the known partition functions under DC [Eq. (8)] as [7]

$$\begin{aligned} Z_F^{WLC}(n,F) &= \int_{\overline{R_Z}} Z^{WLC}(n,\overline{R_Z}) \exp\left(\frac{f R_Z}{k_B T} \right) d\overline{R_Z} \\ &= \int_{\overline{R_Z}} Z^{WLC}(n,\overline{R_Z}) \exp(F\overline{R_Z}) d\overline{R_Z}. \end{aligned} \tag{10}$$

The total partition function for the WLC can be obtained in a manner similar to Eq. (3) for the FJC as

$$Z_{FC}^{WLC}(F) = \sum_{n=0}^{N} Z_{ads}(n) Z_F^{WLC}(n,F). \tag{11}$$

D. Rotational isomeric state model [26]

Modeling the ssDNA backbone as an RIS chain provides a better representation than the FJC or WLC models at the cost of some loss of generality and gain in complexity. Each ssDNA mer consists of six bonds, six bond angles, and six torsion angles [Fig. 1(b)]. We assume that all the lability of the ssDNA comes from its backbone torsions with the bond lengths and bond angles fixed at equilibrium values. The

adhesive interaction between the DNA backbone and the substrate is assigned to the backbone bond that is a part of the sugar ring. For a given conformation of the DNA, the potential energy of each mer is calculated as the sum of six dihedral potentials corresponding to the six dihedral angles [Fig. 1(b)]. (Note that the dihedral angle is the supplement of the torsion angle.) The dihedral potential for a given dihedral angle φ, based on CHARMM force field [27], is given by

$$V(\varphi) = \sum_n K_n[1 + \cos\{n\varphi - \varphi_o\}] \tag{12}$$

where K_n is the n-fold barrier energy, and φ_o is the reference dihedral angle corresponding to the minimum energy state. (See SI Sec. VII for details and values of these parameters [23].)

The dihedral conformations of each torsion are represented by two states (called rotamers or conformers), state 1 and state 2. The 360° dihedral angle domain is divided into two such that the populations of both the domains, p_1 and p_2, are the same, i.e.,

$$p_1 = p_2 = z^{-1}\int_{domain} \exp\left(-\frac{v(\varphi)}{k_B T}\right)d\varphi = 0.5,$$

$$z = \int_0^{2\pi} \exp\left(-\frac{v(\varphi)}{k_B T}\right)d\varphi, \tag{13}$$

where z is the conformational partition function. The dihedral angle corresponding to each state is given by

$$\langle\varphi_i\rangle = (p_i z)^{-1}\int_{domain} \varphi_i \exp\left(-\frac{v(\varphi_i)}{k_B T}\right)d\varphi_i, \quad i = 1,2. \tag{14}$$

Each mer has 2^6 conformations and n mers have 2^{6n} conformations. For each conformation, one can construct the ssDNA backbone and determine the end-to-end distance R_Z. (See SI Sec. VII2 [23,26]) For one mer, the maximum end-to-end distance, which is equal to the contour length of one mer, l_m, is 0.69 nm.

1. Displacement control

Under semi-DC, the partition function $Z^{RIS}(n,\overline{R_Z})$ of a chain n mers long for a given R_Z (or $\overline{R_Z}=\frac{R_Z}{l_m}=\frac{R_Z}{b}$) is equal to number of conformations with the z component of end-to-end distance between R_Z and R_Z+dR_Z and $\int_{\overline{R_Z}} Z(n,\overline{R_Z})d\overline{R_Z} = 2^{6n}$ (note that, by construction, all conformations have the same energy). To evaluate the partition function exactly, one has to construct all possible conformations, i.e, 2^{6n}, which grows extremely rapidly with increasing n. Instead, we approximate the partition function by randomly choosing Q conformations instead of generating them all. Because, all allowed states are equally likely by construction, randomly picking a subset of all conformations introduces no bias for given n. Using these Q conformations, $Z^{RIS}(n,\overline{R_Z})$ is evaluated numerically (see SI Sec. VII3 for more details [23]). $Z^{RIS}(n,\overline{R_Z})$ is scaled by $\frac{2^{6n}}{Q}Z^{RIS}(n,\overline{R_Z})$ such that $\int_{\overline{R_Z}} Z^{RIS}(n,\overline{R_Z})d\overline{R_Z} = \Sigma_{\overline{R_Z}} Z^{RIS}(n,\overline{R_Z}) = 2^{6n}$. Average force is calculated numerically as negative of the derivative of the natural logarithm of the partition function with respect to R_Z. We found that the calculated force profile converges for Q considerably smaller than 2^{6n}. For example, with $n=6$, $Q=6575\times10^5$ gave good convergence.

The total partition function for peeling RIS chain can be evaluated in the same manner as that for FJC and WLC [Eqs. (5) and (9)]:

$$Z_{DC}^{RIS}(\overline{R_Z}) = \sum_{n=0}^{N} Z_{ads}(n) Z^{RIS}(n,\overline{R_Z}). \tag{15}$$

2. Force control

The partition function under FC is determined from the partition functions under DC as for the WLC model. The partition function of n mers long chain is

$$Z_F^{RIS}(n,F) = \int_{\overline{R_Z}} Z^{RIS}(n,\overline{R_Z})\exp\left(\frac{fR_Z}{k_B T}\right)d\overline{R_Z}$$

$$= \int_{\overline{R_Z}} Z^{RIS}(n,\overline{R_Z})\exp(F\overline{R_Z})d\overline{R_Z}, \tag{16}$$

where $F=\frac{fl_m}{k_B T}=\frac{fb}{k_B T}$. The total partition function for peeling an RIS chain under FC is given by

$$Z_{FC}^{RIS}(F) = \sum_{n=0}^{N} Z_{ads}(n) Z_F^{RIS}(n,F). \tag{17}$$

III. RESULTS

Using the three models, we consider peeling for three types of polymer chains: (1) homopolymers A_n, (2) block copolymers A_nB_n, and (3) alternating copolymers $(AB)_n$, where A and B label the identity of each link, each under FC and DC.

A. Homopolymers A_n

For an N mers long homopolymer A_n, all mers are alike and the partition function of the adsorbed chain, $Z_{ads}(n)$ becomes $\exp\{(N-n)\Gamma\}$. The results for the homopolymer modeled as the three polymer chains are discussed below.

1. FJC model for A_n

The sum in Eq. (3) for an FJC A_n is a geometric series that can be evaluated exactly to obtain the partition function [14] (SI Sec. III [23]).

$$Z_{FC}^{FJC}(F) = \exp(\Gamma N)\frac{1-\exp[(X-\Gamma)(N+1)]}{1-\exp(X-\Gamma)}; \tag{18}$$

$$P(n) = \frac{\exp[nX + (N-n)\Gamma]}{Z}. \tag{19}$$

With this exact expression for the partition function, we have obtained by ensemble averaging exact closed-form for-

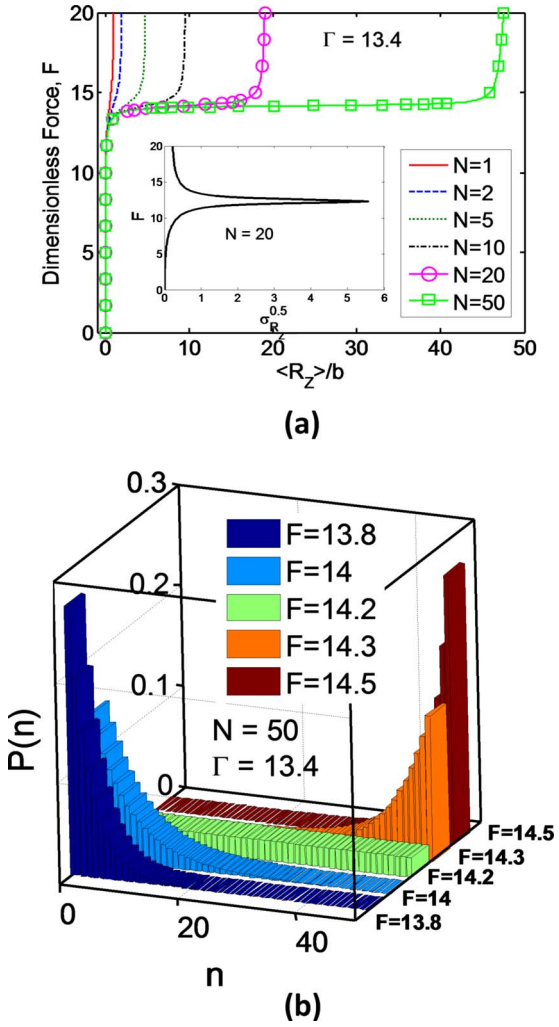

FIG. 2. (Color online) (a) Dimensionless force, F, versus the normalized (average) end-to-end distance, $\langle R_Z\rangle/b$, as a function of chain length. It is evident that for chains longer than 10 links, desorption is resisted by a steady peel force. Inset shows that fluctuations in $\langle R_Z\rangle/b$ are peaked at the peeling force. (b) Probability distribution function $P(n)$ of the FJC for varying dimensionless force. $P(n)$ reaches a constant value of $1/(N+1)$ when Eq. (1) ($F=14.2$, the peeling force for long chains) is satisfied, which means that all states are equally likely. $b=0.69$ nm and $\Gamma=13.4$ [poly(thymine) on graphite].

mulas for average end-to-end displacement and number of links, $\langle R_Z\rangle$ and $\langle n\rangle$, and their fluctuations, $\sigma_n^{0.5}$ and $\sigma_{R_Z}^{0.5}$ (see SI Sec. III for derivations [23]).

$$\langle n\rangle = \frac{r}{1-r} - \frac{(N+1)r^{N+1}}{1-r^{N+1}}; \quad r = \exp(X-\Gamma), \tag{20}$$

$$\frac{\langle R_Z\rangle}{b} = \left(\coth F - \frac{1}{F}\right)\langle n\rangle, \tag{21}$$

$$\langle n^2\rangle = \frac{\exp(N\Gamma)}{Z}\left[-\frac{(N+1)^2 r^{N+1}}{1-r} + \frac{r(1-(2N+3)r^{N+1})}{(1-r)^2} + \frac{2r^2(1-r^{N+1})}{(1-r)^3}\right], \tag{22}$$

$$\frac{\langle R_z^2\rangle}{b^2} = \left[1 + \frac{1}{F^2} - \coth^2 F\right]\langle n\rangle + \left(\coth F - \frac{1}{F}\right)^2\langle n^2\rangle, \tag{23}$$

$$\sigma_n^{0.5} = [\langle n^2\rangle - \langle n\rangle^2]^{0.5}; \quad \sigma_{R_Z}^{0.5} = [\langle R_Z^2\rangle - \langle R_Z\rangle^2]^{0.5}. \tag{24}$$

Note that expression for average displacement as a function of force (21) is in the form of the Langevin function times the average number of desorbed links. Figure 2(a) plots force versus average extension $\langle R_Z\rangle$ for chains of varying number of links N, $b=0.69$ nm and $\Gamma=13.4$, parameters corresponding to poly(thymine) adsorbed on graphite [14]. For $N>10$, as observed experimentally [5,9,10,14], peeling occurs under a steady force. Fluctuations in $\langle R_Z\rangle$ for the chain with 50 links, shown in Fig. 2(a) inset, reach a maximum at $X^*=\Gamma^*$. For this condition, it follows immediately from Eq. (19) that the probability distribution $P(n)$ is uniform, $1/(N+1)$. Figure 2(b) shows probability distributions for applied force in the vicinity of the peeling force F^*. If $(X<X^*=\Gamma)$, corresponding to $F<F^*$, the distribution is asymmetric with mode of $n=0$, while if $(X>X^*=\Gamma)$, corresponding to $F>F^*$, the distribution is asymmetric with mode of $n=N$. This confirms that the condition $(X=X^*=\Gamma)$, Eq. (1), is properly interpreted as the onset of peeling under FC.

Under DC we have not found it possible to simplify Eq. (5) further because the probability distribution for end-to-end distance, $W(n,r)$, itself is known only as the unwieldy Eq. (4) [6,7,21]. We evaluate $Z_{DC}^{FJC}(R_Z)$ numerically and the average force $\langle f\rangle$ by numerical differentiation of the natural logarithm of the partition function with respect to R_Z, keeping T and Γ fixed.

$$\langle f\rangle = -k_B T \left.\frac{\partial \ln Z_{DC}(R_Z)}{\partial(R_Z)}\right|_{T,\Gamma} \quad \text{or} \tag{25}$$

$$\langle F\rangle = -b \left.\frac{\partial \ln Z_{DC}(R_Z)}{\partial(R_Z)}\right|_{T,\Gamma}.$$

The average quantity $\langle n\rangle$ is calculated by numerical ensemble averaging.

Figure 3(a) shows the predicted force during peeling for poly(thymine) with $N=50$ in strict- and semi-DC. Also shown is the predicted (nearly steady) force under FC. Both DCs show that even *equilibrium* peeling of the chain under these conditions occurs *link-by-link*. Note also the stepwise increase in $\langle n\rangle$ with increasing R_Z, and the fact that the force response prior to each peak can be fit by the FJC-Langevin force response for a chain with the corresponding number of links. For strong adhesion (several k_BT per base), when R_Z/b is small, the removal of an extra base is achieved only at the expense of significantly stretching the chain beyond the peel force predicted under FC. When more than about 25 links are

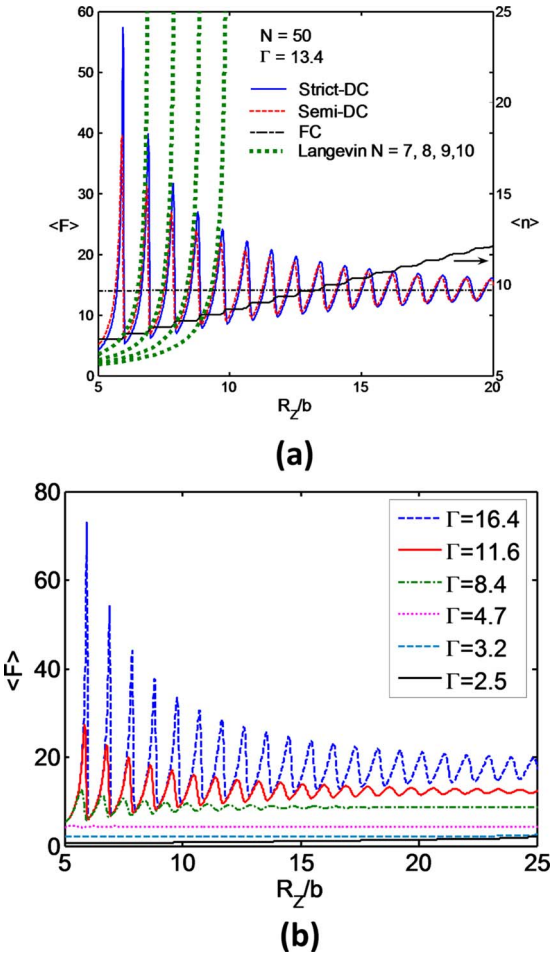

FIG. 3. (Color online) (a) Average dimensionless force $\langle F\rangle$ and average number of desorbed links $\langle n\rangle$ as a function of separation R_Z/b during peeling of poly(thymine) from graphite with $N=50$, $\Gamma=13.4$, and $b=0.69$ nm under strict- and semi-DC. (b) Effect of adhesion Γ on force spikes.

desorbed, the variation in force about the peel force reduces, eventually converging to the FC prediction. The displacements shown in Fig. 3(a) are within an experimentally accessible range [14] and force spikes are considerably larger than experimental fluctuations, suggesting that these should be measurable with a sufficiently stiff loading system. Figure 3(b) shows that the larger the adhesion the larger is the force spike, which implies that it carries information about the base being peeled. Now we ask the following questions: are the predictions model dependent? How do force spikes decay with increasing number of desorbed links? Is it possible to identify the sequence of bases by peeling under DC? In the next few sections, we try to answer these questions.

2. Peeling a WLC or RIS homopolymer, A_n

For the case of WLC and RIS models, the average force under DC can be obtained by taking the natural logarithm of the partition function with respect to R_Z, keeping T and Γ fixed, as in the FJC case [Eq. (25)].

$$\langle F\rangle = -\left.\frac{\partial \ln Z^{WLC}_{DC\_DC}(\overline{R_Z})}{\partial(\overline{R_Z})}\right|_{T,\Gamma} \quad \text{or} \tag{26}$$

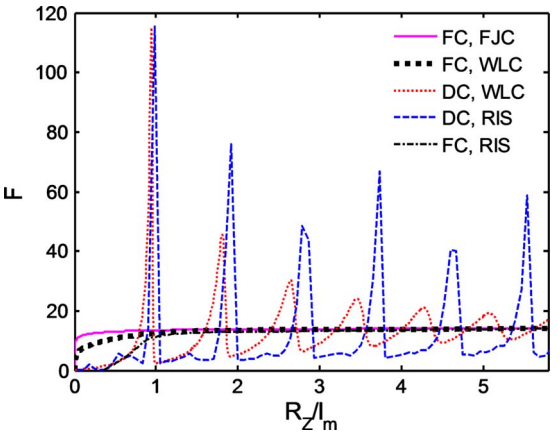

FIG. 4. (Color online) Comparison of force-displacement curves under DC and FC for WLC and RIS models with $l_m=b=n_{pp}l_p=0.69$ nm and $n_{pp}=2$. These are based on a measured peel force of 85 pN for poly(thymine) [14], for which, $\Gamma_{FJC}=13.4$, $\Gamma_{WLC}=11.7$ and $\Gamma_{RIS}=14.2$ were used.

$$\langle F\rangle = \left.\frac{\partial \ln Z^{RIS}_{DC\_DC}(\overline{R_Z})}{\partial(\overline{R_Z})}\right|_{T,\Gamma}.$$

The average end-to-end distance R_Z (or $\overline{R_Z}$) under FC can be calculated using ensemble averaging. Using Eqs. (10) and (11) for WLC and Eqs. (16) and (17) for RIS, we have

$$\langle \overline{R_Z}\rangle = \frac{1}{Z^{WLC}_{FC}(F)}\sum_{n=0}^{N} \times\left\{\exp[(N-n)\Gamma]\int_{\overline{R_Z}} \overline{R_Z} Z^{WLC}(n,\overline{R_Z})\exp(F\overline{R_Z})d\overline{R_Z}\right\}, \tag{27}$$

$$\langle \overline{R_Z}\rangle = \frac{1}{Z^{RIS}_{FC}(F)}\sum_{n=0}^{N} \times\left\{\exp[(N-n)\Gamma]\int_{\overline{R_Z}} \overline{R_Z} Z^{RIS}(n,\overline{R_Z})\exp(F\overline{R_Z})d\overline{R_Z}\right\}. \tag{28}$$

Equations (26)–(28) are evaluated numerically.

The predictions of WLC and RIS models under DC and FC (Fig. 4) are consistent with those of the FJC model suggesting that there will be measurable spikes in force under DC and peeling under steady force for FC. The results of the WLC model are not affected significantly on varying the persistence length within the experimentally measured range. In Fig. 4, we set persistence length to be half of the Kuhn length, i.e., $l_p=l_m/2=0.345$ nm and $n_{pp}=2$.Values for the dimensionless adhesion for the models are chosen so that the peeling occurs at a force of 85 pN as observed experimentally for peeling poly(thymine) [14]. The adhesion for FJC, WLC, and RIS models are 13.4, 11.7, and 14.2, respectively. The results of Figs. 3 and 4 suggest that adhesion between ssDNA bases and graphite is sufficient that there would be force spikes in the equilibrium peeling response. Differences

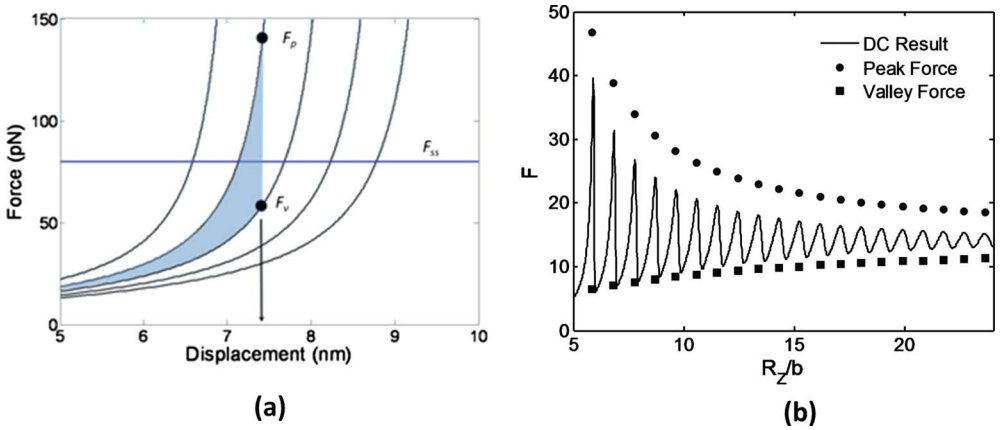

FIG. 5. (Color online) (a) Force-displacement response of FJCs with the same Kuhn length but different numbers of links, 12–16 from left to right. The transition from 13 to 14 peeled links occurs at a critical value of displacement chosen such that the release in stretching free energy, given by the shaded area, equals the increase in adhesion energy. (b) Decay in force spikes with chain length for $\Gamma = 13.4$. The peak and valley forces are shown in circles and squares, respectively. The solid line represents the force-displacement result under semi-DC.

in the magnitude of force spikes and their locations between the three models are due to the differences in their stretching behaviors at large extensions. Spikes in the FJC and RIS models are more prominent than in the WLC model.

However, the overall phenomenon of force spikes in the equilibrium response appears in all three models, which gives some confidence that this prediction is robust. Moreover, Fig. 3(b) shows that it is quite sensitive to the value of adhesion. Some differences follow simply from the models. For example, in case of RIS, stretching characteristic is observed under FC before the first link desorbs because of the first five nonadhesive bonds since the adhesion is incorporated in the sixth bond that is a part of sugar ring [Fig. 1(b)].

3. Decay of force spikes

During peeling of an FJC with discrete adhesion sites under DC, our equilibrium model predicts that the force will display spikes (Figs. 3 and 4). These spikes decay as the length of the peeled portion of the chain increases, eventually to a steady-state force F_{ss} as predicted under FC. If the phenomenon of force spikes is to be realized experimentally, potentially to read the sequence of a strand of DNA by peeling, it is important to understand more simply why the force spikes appear, and how they decay with chain length. Here we develop a simple two-state model for this purpose.

Figure 5(a) shows five curves representing the force-displacement response of FJCs with different numbers of links (12–16 from left to right) and the same Kuhn length (0.69 nm). Let us assume that under DC the system has to choose between two adjacent states with different numbers of peeled links. For example, consider the transition from 13 to 14 peeled links in Fig. 5(a) to occur at a critical displacement. The critical displacement is decided by the balance between the stretching free energy loss given by the shaded area in Fig. 5(a) and the adhesion free energy penalty minus the entropic free energy increase due to desorption of one additional link.

Let, δ be the applied displacement at which the transition from n to $n+1$ peeled links occurs. Forces f_p and f_v are required to maintain this displacement for chains with n and $n+1$ links, respectively. The free energy of the chain N links long with n links desorbed subjected to a displacement δ is

$$G(n) = \int_0^{\delta} f(n,\delta)d\delta' - nk_BT\ln[4\pi] - (N-n)b\gamma, \quad (29)$$

where the first term gives the strain energy or the area under the force-displacement curve, the second term is the entropic contribution, and the third term is the adhesion energy. The force on the chain as a function of displacement is given by inverse Langevin approximation [28,29].

$$f(n,\delta) = \frac{\delta k_BT}{nb^2}\left[\frac{3-(\delta/nb^2)}{1-(\delta/nb^2)}\right]. \quad (30)$$

It is convenient to introduce the normalization

$$\bar{\delta} = \frac{\delta}{b}; \quad \bar{G} = G/k_BT. \quad (31)$$

From Eqs. (29)–(31), the free energy of the chain is

$$\bar{G}(n) = n\left[\frac{1}{2}\left(\frac{\bar{\delta}}{n}\right)^2 - \ln\left\{1-\left(\frac{\bar{\delta}}{n}\right)^2\right\}\right] + n\{\Gamma - \ln(4\pi)\} - N\Gamma. \quad (32)$$

The approximate condition for the transition from n *to* $n+1$ peeled links is that

$$\bar{G}(n) = \bar{G}(n+1),$$

or

$$n\left[\frac{1}{2}\left(\frac{\bar{\delta}}{n}\right)^2 - \ln\left\{1-\left(\frac{\bar{\delta}}{n}\right)^2\right\}\right] - (n+1)\left[\frac{1}{2}\left(\frac{\bar{\delta}}{n+1}\right)^2 - \ln\left\{1-\left(\frac{\bar{\delta}}{n+1}\right)^2\right\}\right] = \Gamma - \ln(4\pi). \quad (33)$$

Equation (33) gives the critical displacement δ correspond-

ing to the transition from n to $n+1$ peeled links. The peak and valley forces, f_p and f_v (F_p and F_v), can obtained from Eq. (30).

The peak and valley forces predicted by the simple transition model shown as the black circles and squares in Fig. 5(b) are in reasonably good agreement with the FJC model under semi-DC. Note that the full force-displacement response was calculated under semi-DC whereas the simple model uses the Inverse Langevin function for strict-DC, which accounts for some of the discrepancy. See SI Sec. IV [23] for more details, including a look at the problem using an exact Langevin relation. We show there that the peak force scales approximately as $f_p \sim \exp([\Gamma - \ln 4\pi]/n)$, highlighting the strong sensitivity to adhesion, Γ.

The remaining results have all been obtained using the FJC model.

B. Block copolymers

Since the adhesion free energy of homopolymers depends significantly on the identity of the base, anticipating a change in peeling force in the vicinity of the interface between the two blocks, we first consider the case of block polymers A_nB_n, with different adhesion free energies ($\Gamma_A \neq \Gamma_B$) but with the same Kuhn lengths. Under FC, by extending the approach used for homopolymers, we have obtained exact closed-form results for the partition function, probability density functions, and average displacement and n. Here we provide the final results, see SI Sec. V [23] for details.

$$Z_{FC}^{FJC}(F) = \exp(N_A\Gamma_A + N_B\Gamma_B)\left[\frac{1 - r_A^{N_A+1}}{1 - r_A} + r_A^{N_A}\frac{r_B - r_B^{N_B+1}}{1 - r_B}\right],$$

$$r_i = \exp(X - \Gamma_i); \quad \Gamma_i = \frac{\gamma_i b}{k_B T} \quad i = A,B, \tag{34}$$

$$P(n) = \begin{cases} \dfrac{\exp(N_A\Gamma_A + N_B\Gamma_B) r_A^n}{Z_{FC}^{FJC}} & n \leq N_A \\ \dfrac{\exp(N_A\Gamma_A + N_B\Gamma_B) r_A^{N_A} r_B^{n-N_A}}{Z_{FC}^{FJC}} & n > N_A \end{cases}, \tag{35}$$

$$\langle n \rangle = \frac{\exp(N_A\Gamma_A + N_B\Gamma_B)}{Z}\left[\frac{(N_A+1)r_A^{N_A+1}}{1 - r_A} + \frac{r_A(1 - r_A^{N_A+1})}{(1 - r_A)^2} + r_A^{N_A}\left(N_A\frac{r_B - r_B^{N_B+1}}{1 - r_B} - \frac{(N_B+1)r_B^{N_B+1}}{1 - r_B} + \frac{r_B(1 - r_B^{N_B+1})}{(1 - r_B)^2}\right)\right], \tag{36}$$

$$\langle R_Z \rangle = b\left(\coth F - \frac{1}{F}\right)\langle n \rangle. \tag{37}$$

Figure 6 shows the predicted peel forces depend on whether the weaker [$\Gamma_A < \Gamma_B$, Fig. 6(a)] or stronger [$\Gamma_A > \Gamma_B$, Fig. 6(b)] binding strand peels first [the values of Γ_A, Γ_B correspond to reported measurements on poly(thymine) and poly(cytosine) on graphite [14]]. If the weaker binding strand occurs first, strand A peels first at $X = \Gamma_A$; strand B then peels at $X = \Gamma_B$. The transition between these two steps occurs over 2–5 links, indicating it would be difficult to read the sequence under FC. If the stronger binding strand is required to peel first, $\Gamma_A > \Gamma_B$, the equilibrium model under FC predicts peeling at a single force representative of a homopolymer with an effective adhesion free energy, $\Gamma_{eff} = \frac{N_A\Gamma_A + N_B\Gamma_B}{N_A + N_B}$. We expect that the prediction for $\Gamma_A > \Gamma_B$ will not be realized experimentally since it depends on all states for n being equally accessible.

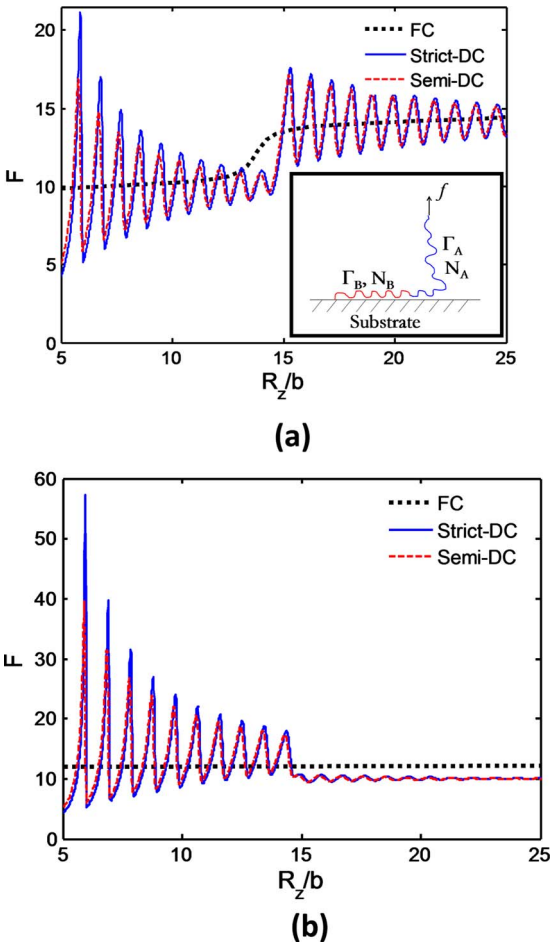

FIG. 6. (Color online) Peel profiles for block polymers in DC. (a) $\Gamma_A < \Gamma_B$. (b) $\Gamma_A > \Gamma_B$. $\Gamma_A = 13.4$, and $\Gamma_B = 9.5$ [poly(thymine) and poly(cytosine), respectively]. Inset in (a) shows the schematic representation of block copolymer peel. $N_A = N_B = 15$ and $b = 0.69$ nm.

The results for block copolymers under DC are also shown in Fig. 6 for the two cases: $\Gamma_A < \Gamma_B$ and $\Gamma_A > \Gamma_B$. As in the case of the homopolymer, we find that peeling occurs link-by-link. The force peaks for the stronger binding base are significantly higher than for its weaker binding cousin and the transition between the two occurs within a single link.

C. Alternating copolymers

The fact that under DC the transition in force occurs over one link prompts us to analyze the peeling an alternating polymer of type $(AB)_N$, again with Γ_A, Γ_B values for poly-

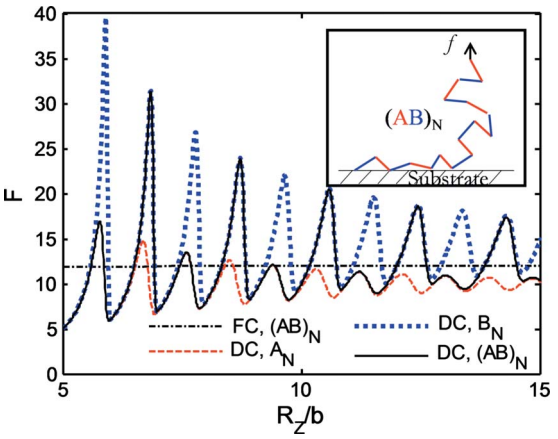

FIG. 7. (Color online) Peel profile for an alternating copolymer $(AB)_N$ shows that under FC we expect peeling under a steady force. Under DC, the polymer peels link-by-link and each spike in force is representative of the identity of the link currently being desorbed. Results are for semi-DC with $N=50$, $b=0.69$ nm, $\Gamma_A=9.5$ and $\Gamma_B=13.4$, representative of poly(cytosine) and poly(thymine) on graphite, respectively.

(cytosine) and poly(thymine) on graphite [14]. We present the final results only; see SI Sec. VI [23] for details.

$$Z_{FC}^{FJC}(F) = \exp(N\Gamma_A + N\Gamma_B) \times \left[\frac{1-(r_A r_B)^{N+1}}{1-r_A r_B} + \frac{r_A r_B - (r_A r_B)^{N+1}}{r_B(1-r_A r_B)}\right], \quad (38)$$

$$\langle n\rangle = \frac{\exp(N\Gamma_A + N\Gamma_B)}{Z_{FC}^{FJC}}\left[2\left(1+\frac{1}{r_B}\right)\left\{-\frac{(N+1)(r_A r_B)^{N+1}}{1-r_A r_B} + \frac{r_A r_B[1-(r_A r_B)^{N+1}]}{(1-r_A r_B)^2}\right\} - \frac{r_A r_B - (r_A r_B)^{N+1}}{r_B(1-r_A r_B)}\right], \quad (39)$$

$$\langle R_Z\rangle = b\left(\coth F - \frac{1}{F}\right)\langle n\rangle. \quad (40)$$

Under FC the model predicts that the measured peel force is nearly a constant (Fig. 7), representative of the average adhesion free energy of the polymer. However, under semi-DC, we predict that, even under equilibrium, peaks in the force response carry the signature of the identity of each base (Fig. 7). (Results for strict-DC are nearly identical and not shown for the sake of clarity.)

IV. SUMMARY AND CONCLUSIONS

We have analyzed the equilibrium peeling of single-stranded DNA off graphite as peeling of a polymer chain with discrete adhesion sites under force or displacement control strongly adsorbed to a frictionless substrate. All three polymer models used to represent ssDNA, namely, freely jointed chain, wormlike chain, and rotational isomeric state models, predict similar peeling response under force and displacement control. For homopolymers under FC the FJC model predicts peeling under a steady force and provides a relation between it and the underlying adhesion free energy. This is in good agreement with a number of single-molecule peeling experiments for ssDNA on graphite and for other polymer-substrate combinations, suggesting that the basic hypotheses of equilibrium and frictionless substrates are often satisfied. For FJC under FC, we have obtained exact closed-form results for the partition function, the force-displacement relation, and fluctuations in length and number of bound links. All three models under DC predict peeling to occur base-by-base for short strands with attendant spikes in force that are significantly greater than typical force fluctuations and therefore ought to be measurable. Analysis of block and alternating copolymers suggests that under DC these force spikes carry information about the underlying sequence of the ssDNA, which might thus be measurable with a sufficiently stiff loading system. While the discussion has centered around peeling of ssDNA from graphite, because our FJC model is a generic model for several polymers, the model and conclusions drawn from it can be extended to peeling of other chainlike molecules [23].

ACKNOWLEDGMENTS

This work was supported by the National Science Foundation Grant No. CMS-0609050. The authors have benefited from several discussions with C-Y. Hui, T. Tang, and D. Vezenov.

[1] S. B. Smith, L. Finzi, and C. Bustamante, Science **258**, 1122 (1992).
[2] S. B. Smith, Y. J. Cui, and C. Bustamante, Science **271**, 795 (1996).
[3] E. L. Florin, V. T. Moy, and H. E. Gaub, Science **264**, 415 (1994).
[4] M. Rief, F. Oesterhelt, B. Heymann, and H. E. Gaub, Science **275**, 1295 (1997).
[5] X. Chatellier, T. J. Senden, J. F. Joanny, and J. M. di Meglio, Europhys. Lett. **41**, 303 (1998).
[6] L. R. G. Treloar, Trans. Faraday Soc. **42**, 77 (1946).
[7] P. J. Flory, *Statistical Mechanics of Chain Molecules* (Interscience Publishers, New York, 1969).
[8] H. Clausen-Schaumann, M. Seitz, R. Krautbauer, and H. E. Gaub, Curr. Opin. Chem. Biol. **4**, 524 (2000).
[9] C. Friedsam, A. D. Becares, U. Jonas, M. Seitz, and H. E. Gaub, New J. Phys. **6**, 9 (2004).
[10] C. Friedsam, H. E. Gaub, and R. R. Netz, Europhys. Lett. **72**, 844 (2005).
[11] L. Sonnenberg, J. Parvole, O. Borisov, L. Billon, H. E. Gaub, and M. Seitz, Macromolecules **39**, 281 (2006).
[12] L. Sonnenberg, J. Parvole, F. Kuhner, L. Billon, and H. E. Gaub, Langmuir **23**, 6660 (2007).
[13] K. Kendall, J. Phys. D **4**, 1186 (1971).

[14] S. Manohar, A. R. Mantz, C.-Y. Hui, A. Jagota, and D. V. Vezenov, Nano Lett. **8**, 4365 (2008).
[15] S. J. Sowerby, C. A. Cohn, W. M. Heckl, and N. G. Holm, Proc. Natl. Acad. Sci. U.S.A. **98**, 820 (2001).
[16] S. J. Sowerby, C.-M. Mörth, and N. G. Holm, Astrobiology **1**, 481 (2001).
[17] L. I. Klushin, A. M. Skvortsov, and A. A. Gorbunov, Usp. Fiz. Nauk **168**, 719 (1998).
[18] C. Bustamante, Z. Bryant, and S. B. Smith, Nature (London) **421**, 423 (2003).
[19] A. Janshoff, M. Neitzert, Y. Oberdorfer, and H. Fuchs, Angew. Chem. Int. Ed. **39**, 3212 (2000).
[20] M. Rubinstein and R. H. Colby, *Polymer Physics* (Oxford Univeristy Press, New York, 2003), pp. 74–76.
[21] L. R. G. Treloar, *The Physics of Rubber Elasticity* (Oxford University Press, London, 1958), pp. 100–113.
[22] L. Rayleigh, Philos. Mag. **37**, 321 (1919).
[23] See supplementary material at http://link.aps.org/supplemental/10.1103/PhysRevE.81.021805 for detailed derivations and explanations of results presented in this article.
[24] C. Bustamante, J. F. Marko, E. D. Siggia, and S. Smith, Science **265**, 1599 (1994).
[25] J. F. Marko and E. D. Siggia, Macromolecules **28**, 8759 (1995).
[26] W. L. Mattice and U. W. Suter, *Conformational Theory of Large Molecules* (Wiley, New York, 1994).
[27] N. Foloppe and A. D. MacKerell, J. Comput. Chem. **21**, 86 (2000).
[28] A. Cohen, Rheol. Acta **30**, 270 (1991).
[29] P. T. Underhill and P. S. Doyle, J. Rheol. **49**, 963 (2005).